

Surface electrophoresis of ds-DNA across orthogonal pair of surfaces

Cite as: Appl. Phys. Lett. **98**, 164102 (2011); <https://doi.org/10.1063/1.3565238>

Submitted: 23 November 2010 . Accepted: 15 February 2011 . Published Online: 19 April 2011

Arnab Ghosh, Tarak K. Patra, Rishi Kant, Rajeev Kr. Singh, Jayant K. Singh, Shantanu Bhattacharya, et al.



View Online



Export Citation

ARTICLES YOU MAY BE INTERESTED IN

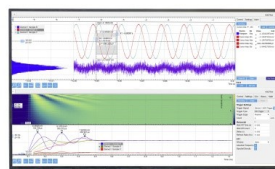
[Electrical characterization of DNA molecules in solution using impedance measurements](#)
Applied Physics Letters **92**, 143902 (2008); <https://doi.org/10.1063/1.2908203>

[Localization and stretching of polymer chains at the junction of two surfaces](#)
The Journal of Chemical Physics **140**, 204909 (2014); <https://doi.org/10.1063/1.4878499>

[Vapor-liquid phase coexistence and transport properties of two-dimensional oligomers](#)
The Journal of Chemical Physics **137**, 084701 (2012); <https://doi.org/10.1063/1.4747195>

Challenge us.

What are your needs for
periodic signal detection?



Zurich
Instruments

Surface electrophoresis of ds-DNA across orthogonal pair of surfaces

Arnab Ghosh,¹ Tarak K. Patra,² Rishi Kant,¹ Rajeev Kr. Singh,¹ Jayant K. Singh,² and Shantanu Bhattacharya^{1,a)}

¹Department of Mechanical Engineering, Indian Institute of Technology, Kanpur 208016, India

²Department of Chemical Engineering, Indian Institute of Technology, Kanpur 208016, India

(Received 23 November 2010; accepted 15 February 2011; published online 19 April 2011)

A gel free microchannel device made up of polydimethyl siloxane is fabricated for the surface based electrophoresis of double stranded deoxy-ribonucleic acid (DNA) molecules. In the presence of directional external electric field, DNA fragments near the corners of the microchannel are found to separate faster as compared to those over the base of the channel. This is in spite of the reduction in the mobility of molecules over the channel corners. We performed coarse grained molecular dynamics simulations which reveal that, though the adsorption energy of the DNA fragments increases near the corner, it is the increase in the relative mobility which enhances the separation of the fragments over the corner. © 2011 American Institute of Physics. [doi:10.1063/1.3565238]

Fractionation of ds-DNA based on different molecular lengths by passing them through a sieving medium has been regularly explored for all diagnostics. Some of the widely used methods include slab-gel electrophoresis,¹ zone electrophoresis,^{2,3} capillary electrophoresis⁴⁻⁷ in microcapillaries, microfabricated channel arrays, etc.^{8,9} Fragment sizes above 10 kbp (kilo base pairs) are resolved very poorly by the above bulk electrophoresis techniques.⁵ Thus, new schemes for DNA fractionation have emerged involving electrostatic interactions between nucleic acid molecules and surfaces using its inherent chemical, topological, or structural properties,¹⁰⁻¹³ as demonstrated for the first time by Pernodet *et al.*¹⁰ over a perfectly flat silicon wafer and later by Han and Craighead.¹⁴ Literature shows the influence of various parameters like electric field intensity, ionic strength, and migration distances on the mobility of ds-DNA as they are transported along surfaces.¹⁵ Lee and Kuo¹⁶ fabricated a gel-free microchannel electrophoresis device for fractionating larger DNA fragments (3.5–21.2 kbp) where they chemically modified the channel's bottom surface. The process although widely explored has not been fully understood.

In this letter, we have investigated the surface electrophoresis process for ds-DNA in polydimethyl siloxane (PDMS) microchannels. A peculiar behavior of ds-DNA is observed as they move along the channel corners instead of the channel base in a few trials. The channel length and time needed for fractionating a 1 kb ladder decreased substantially along the channel corners as compared to the base. In other words, orthogonally placed pair of surfaces (channel corners) is found to be more favorable for the fractionation process in comparison to flat surfaces (channel base). We have utilized molecular dynamics (MD) simulations to understand the physics of interaction of the ds-DNA with the surface to explain the above behavior.

The microchannel electrophoresis device for our experiments was fabricated in PDMS by using a CO₂ laser (Epilog Legend Mini 24 Laser, 30 W, 1200 dpi) etched pattern on a poly-methyl methacrylate substrate. The features formed over the acrylic substrate were replicated using PDMS after proper surface treatment with a mold release agent (hexamethyl disilazane) (Fig. 1).²⁰ The bottom side of the PDMS

slab containing the replicated microchannel on its top surface was placed over a glass slide. The Platinum electrodes were placed 2 cm apart at both ends of the PDMS channel. A 0.5 μ l drop of 1 kb DNA ladder solution (1–10 kbp, ds-DNA fragments, concentration 500 μ g/ml, M/S Bangalore Genie, India) was loaded into the feed reservoir and air dried for 10 min multiple times until a total of 2 μ l of sample solution was loaded.¹⁶ After this, 1 \times TAE (triacetate) buffer was poured in the buffer chamber so that the electrodes and the whole channel was completely immersed in the buffer solution. Labeling was done by adding 20 μ g/ml of Ethidium bromide to this buffer solution. The electrodes were activated by a power source supplying 24 V dc. The images of the labeled stains were acquired by a charge coupled device camera and a microscope (Nikon 80i) using tetramethyl rhodamine isothiocyanate filter, excitation 525–540 nm, emission 605–655 nm, with a 4 \times objective (field of view -3.76×2.67 mm²). The microscope stage was precisely positioned at different points across the channel to generate temporal behavior at fixed locations and also the spatial behavior of the moving DNA stains. The mobility studies were performed by identification of the boundaries of the DNA stains using IMAGE-J analysis and MATLAB, and subsequently locating and tracing the motion of the center of mass (CM trace method).¹⁷ The motion of DNA fragments of sizes ranging from 1 to 10 kbp were correspondingly cap-

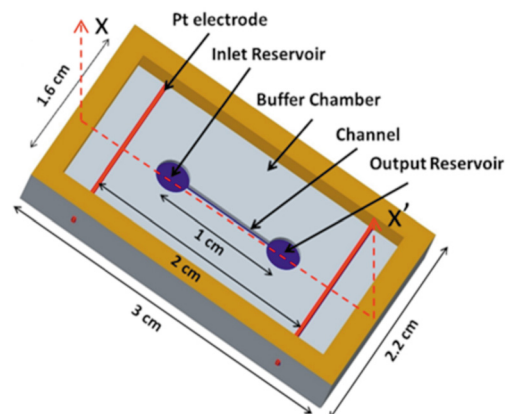


FIG. 1. (Color online) Schematic of the SE device, (dimensions: reservoirs diameter=3 mm, width of channel=400 μ m, depth of features=250 μ m).

^{a)}Electronic mail: bhattach@iitk.ac.in.

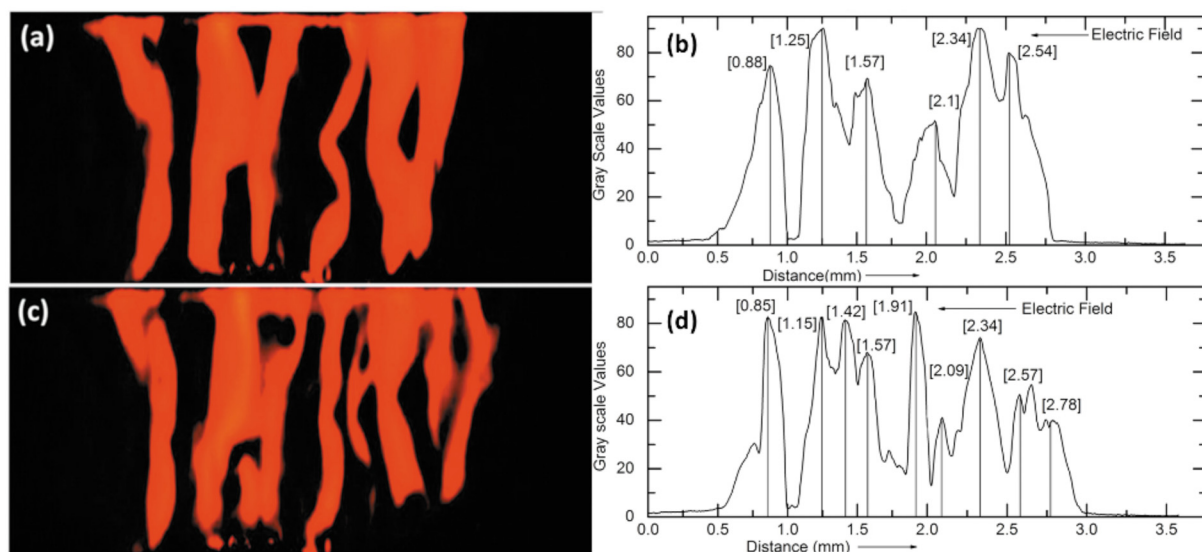


FIG. 2. (Color online) (a) Fragmented ds-DNA at time 8 min and 24 s after the application of electric field across flat surface (channel walls). (b) Corresponding Image J analysis of (a) showing individual peaks identifying the different fragments formulated (the numeric in square brackets represent the abscissa [distance in mm] of the peaks from the left end of the image). (c) Successive snap shot taken after 22 s at the same location as case (a). (d) Corresponding IMAGE-J analysis of (c) done in a similar manner.

tured at various instants of time. The images so acquired were analyzed using IMAGE-J (NIH) which identified the fractionated sizes as peaks (peak trace method). The plotted data of this peak trace method is a characteristic signature of the different sized fragment motion and resembled an electropherogram. All length measurements have been done using image-flow express (M/S Nikon). The time span has been monitored using a stop watch during the electrophoresis process. We compared the mobilities of the various fragments by the CM trace method¹⁷ (reported earlier) and this data was subsequently cross validated with that obtained by peak trace method.

While investigating the fractionation of a 1 kb ds-DNA ladder in our device we have observed distinct fragments formulate after 8 min when these move over the channel base

and 7 min when they move over the channel corners. The mobility information for both the cases is obtained from these intensity plots [Figs. 2 and 3(a)–3(d)] by comparing snapshots taken at different time instances of the moving fragments, without varying the objective spatially. Distances of the distinct peaks, representative of the various fragments, are measured from the left end of the image and are used to calculate the CM of the ladder.²⁰ The total distance traversed by the CM of the ladder is around $31.29 \mu\text{m}$ after a total elapsed time of 22 s (i.e., between the two snapshots at the same spatial location) in the flat surface case. The mobility of the CM is calculated as $1.3 \times 10^{-5} \text{ cm}^2/\text{V s}$ over the channel base and $9.3 \times 10^{-6} \text{ cm}^2/\text{V s}$ over the channel corners. The total distance, from the loading point (center of the reservoir), traversed by the DNA to get fully fragmented in

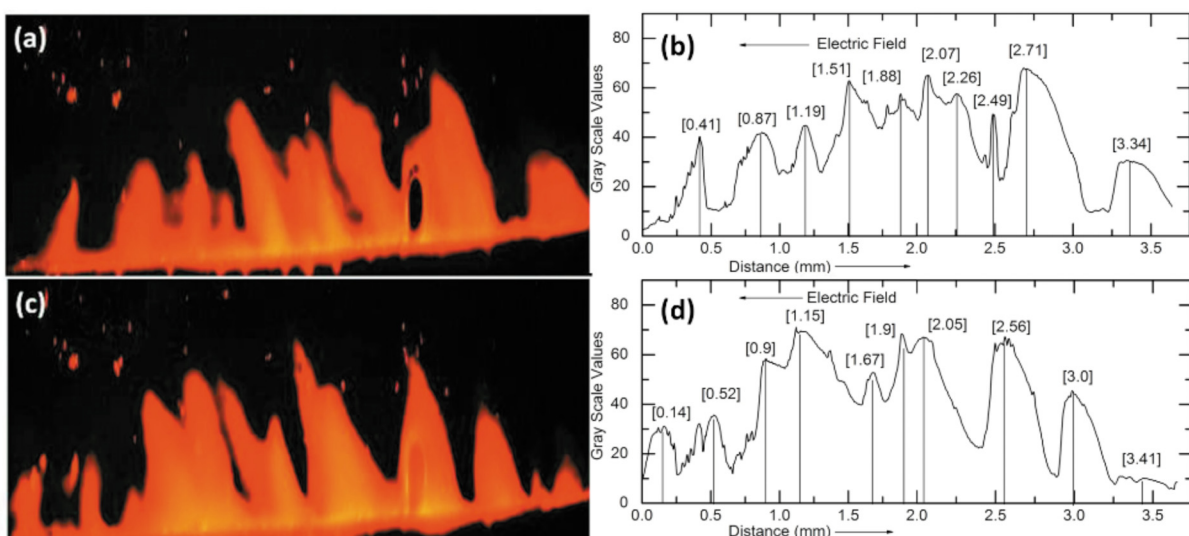


FIG. 3. (Color online) (a) Fragmented ds-DNA at time 7 min after the application of electric field across orthogonal surfaces (channel corners). (b) Corresponding IMAGE-J analysis of case (a) showing individual peaks identifying the different fragments formulated. (c) Successive snap shot taken after 71 s at the same location as (a). (d) Corresponding IMAGE-J analysis of case (c) showing individual peaks identifying the different fragments formulated.

the channel base is observed as 6.8 mm in 9 min and 3.8 mm in case of the channel corner in 7 min. We also calculated the ratio between the spatial spread of the moving fragments and the distance from the loading point traversed by the CM of the ladder at full fragmentation. This ratio is defined as the fragmentation ratio and it is calculated as 0.35 in case of the flat surface and 0.91 (almost three times) for the channel corners. This increase in the fragmentation ratio clearly demonstrates better fragmentation efficiency in case of the orthogonal pair of surfaces as compared to the flat surface. We have validated the differential fragmentation by a dual channel experiment and we observed a similar behavior.²⁰

To examine the physics underlying these observed phenomena, we utilize MD simulations using LAMMPS.¹⁸ DNA particle is represented by a coarse-grain bead-spring model where each bead is a monomer of mass m with an effective charge q . Beads are interacted among each other through a truncated Lennard-Jones (LJ) potential. Adjacent monomers are connected through FENE potential.¹⁹ Surface is modelled as two (111) planes of fcc lattice. LJ Potential is used to represent the interaction between the beads and surface atoms. More details can be found in Ref. 10. Temperature $T = 4.0\epsilon/k_B$ is fixed by coupling the system with a heat bath,¹⁹ and an electric field of 0.02 in unit of $q\sigma E/\epsilon$ is applied. Velocity-verlet algorithm is used to integrate the equation of motion with integration time step $\Delta t = 0.005\tau$ where $\tau = (m\sigma^2/\epsilon)^{1/2}$ is the unit of time. We have considered three cases with number of beads, $N=20, 60,$ and 120.

Ten independent simulations with different initial conformation of the chain are conducted per case for statistically significant results. We observe a loop-train conformation of the DNA chains similar to that observed previously in literature.¹⁰ In the orthogonal surface the trains and loops portion of the DNA latches criss-cross over both the surfaces and develop more number of latch points in comparison to flat surface.²⁰ Adsorption fraction of a 60 bead chain is 0.348 ± 0.06 on flat and 0.519 ± 0.06 being on orthogonal surface.²⁰ We hypothesize that as an orthogonal surface is brought near a looping DNA molecule on an otherwise flat surface some of the portions of the loops would tend to latch over this orthogonal surface. We have also determined the radius of gyration of the adsorbed molecule over both the cases for a number of beads $N=60$ and found that this radius increases from 7.567 AU (absolute units) to 11.266 AU as the molecule is adsorbed over orthogonal pair of surfaces. The increased radius of gyration suggests a general elongation of the molecule from its initial helical confirmation. As the molecules are strongly adsorbed over orthogonal pair of surfaces they would move slowly on application of an external electric field. This behavior is also observed experimentally and reported earlier in Figs. 2 and 3, where the mobility of the ladder, determined from the peak trace method, is reduced from $1.3 \times 10^{-5} \text{ cm}^2/\text{V}$ to $9.3 \times 10^{-6} \text{ cm}^2/\text{V}$ s from the flat surface to the orthogonal surface as is also reflected from MD simulations [Fig. 4]. The plot between the $\log[\mu]$ and the $\log[N]$ indicates an increase in the slope for the orthogonal case which clearly illustrates that the difference in mobility values between $N=20, 60, 120$ is less in flat surface as compared to orthogonal surfaces. This behavior is attributed to the increase in the entropic difference between the chains in the presence of orthogonal surface. This is in agree-

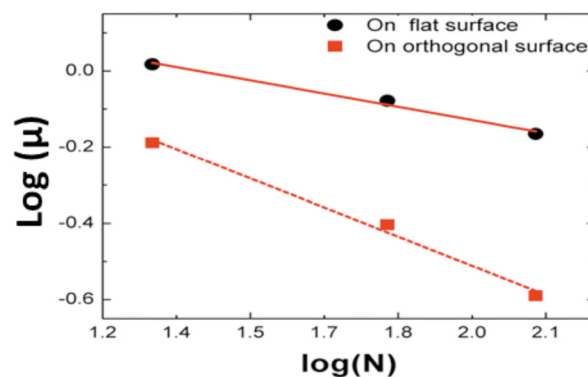


FIG. 4. (Color online) (a) Adsorption for $N=60$ on flat and orthogonal surfaces. Adsorption is defined as the ratio of adsorbed beads and total number of beads of a polymer chain. It shows the adsorption during the system evolution for a span of time for a polymer of size $N=60$.

ment with our experimental observation wherein we notice the fragmentation ratio experimentally to decrease from 0.91 to 0.35 from the orthogonal to the flat surface case. In conclusion, we have observed the fragmentation efficiency of the ds-DNA molecules to substantially increase as they approach an orthogonal pair of surfaces normally found at the corners of rectangular channel geometry.

This work is financially supported by the Department of Biotechnology and the Department of Science and Technology, Government of India and the Dean of Research at the Indian Institute of Technology Kanpur.

- ¹Z. Djouadi, S. Bottani, M. A. Duval, R. Siebert, H. Tricoire, and L. Valentin, *Electrophoresis* **22**, 3527 (2001).
- ²M. G. Janini, R. J. Fisher, L. E. Henderson, and H. J. Issaq, *J. Liq. Chromatogr.* **18**, 3617 (1995).
- ³M. Chiari, M. Nesi, and P. G. Righetti, *Electrophoresis* **15**, 616 (1994).
- ⁴C. Patrick, *Capillary electrophoresis: Theory and Practice* (CRC, London, 1993).
- ⁵S. Bhattacharya, *Economics of advanced trainings, basics, concepts and method* (VDM, Germany, 2008).
- ⁶S. Bhattacharya, N. Chanda, Y. Liu, S. A. Grant, K. Gangopadhyay, D. Gangopadhyay, R. Bashir, P. Sharp, and S. Gangopadhyay, *Journal of Bionanoscience* **2**, 67 (2008).
- ⁷C. B. Tabi, A. Mohamadou, and T. C. Kofané, *Journal of Bionanoscience* **2**, 1 (2008).
- ⁸E. T. Lagally and H. T. Soh, *Crit. Rev. Solid State Mater. Sci.* **30**, 207 (2005).
- ⁹V. M. Ugaz, R. D. Elms, R. C. Lo, F. A. Shaikh, and M. A. Burns, *Philos. Trans. R. Soc. London, Ser. A* **362**, 1105 (2004).
- ¹⁰N. Pernodet, V. Samuilov, K. Shin, J. Sokolov, M. H. Rafailovich, D. Gersappe, and B. Chu, *Phys. Rev. Lett.* **85**, 5651 (2000).
- ¹¹Y. S. Seo, V. A. Samuilov, J. Sokolov, M. Rafailovich, B. Tinland, J. Kim, and B. Chu, *Electrophoresis* **23**, 2618 (2002).
- ¹²Y.-S. Seo, H. Luo, V. A. Samuilov, M. H. Rafailovich, J. Sokolov, D. Gersappe, and B. Chu, *Nano Lett.* **4**, 659 (2004).
- ¹³Y. Kuo and H. H. Lee, *Electrochem. Solid-State Lett.* **4**, H23 (2001).
- ¹⁴J. Han and H. G. Craighead, *Science* **288**, 1026 (2000).
- ¹⁵B. Li, X. Fang, H. Luo, E. Petersen, Y. S. Seo, V. Samuilov, M. Rafailovich, J. Sokolov, D. Gersappe, and B. Chu, *Electrophoresis* **27**, 1312 (2006).
- ¹⁶H. H. Lee and Y. Kuo, *Jpn. J. Appl. Phys.* **47**, 2300 (2008).
- ¹⁷A. Ghosh, D. Singh, T. Kumar Patra, J. K. Singh, R. Gurunath, and S. Bhattacharya, *Proceedings of the 2009 AIChE Annual Meeting*, Nashville, TN.
- ¹⁸S. J. Plimpton, *J. Chem. Phys.* **117**, 1 (1995).
- ¹⁹G. S. Grest and K. Kremer, *Phys. Rev. A* **33**, 3628 (1986).
- ²⁰See supplementary material at <http://dx.doi.org/10.1063/1.3565238> for figures S1–S6.